Spatial and Spatiotemporal Patterns in the Ionic Brusselator

A. F. Münster[b], P. Hasal[a], D. Šnita[a] and M. Marek[a]

a) Prague Institute of Chemical Technology,
Department of Chemical Engineering,
Technická 5, 166 28 Prague 6, Czech Republic.
E-Mail: hasalp@vscht.cz, dali@vscht.cz, marek@vscht.cz

b) Institute of Physical Chemistry, University of Würzburg,
Marcusstr. 9-11, 8700 Würzburg, FRG.
E-Mail: muenster@phys-chemie.uni-wuerzburg.dbp.de

Abstract

The effects of ionic charge and of an externally applied electric field have been studied both for the simplified (electrical field intensity is constant in space) and for the first time also for the full (spatial electrical field intensity and charge variations considered) ionic Brusselator models. Consideration of ions instead of neutral reaction components causes shifts in the location of bifurcation points of spatial patterns and strongly affects the amplitude of the observed patterns. An imposed electrical field can change the symmetry of patterns. Variations in the field strength may also change fluxes at the boundaries. If the externally imposed field strength is varied in a cyclic fashion the fluxes at the boundaries display hysteresis under certain conditions. In the full ionic Brusselator model an imposed electrical field of certain intensity causes stationary patterns to turn into travelling waves. In the simplified model no field induced waves were observed. When zero-diffusive flux boundary conditions are used, oscillatory behaviour of spatial patterns and bistability of fluxes at the system boundaries occur at low values of imposed electric currents. Coexistence of steady and oscillatory patterns along the system coordinate was found at high intensities of the applied electrical field.

Introduction

Recent observations of patterns generated via the Turing instability in chemical reaction-diffusion systems (Castets *et al* 1990, Ouyang and Swinney 1991a,b, Noszticius *et al* 1987, Kshirsagar *et al* 1991) focussed the interest on stationary spatial patterns. However, still a little is known about the effects of electric charge of some components and of an externally applied electrical field. Equations describing the effects of electrical field on wave propagation were derived and qualitative experiments confirming the stopping and annihilation of waves in the reaction mixture of the Belousov-Zhabotinski (BZ) reaction were performed (Schmidt and Ortoleva 1977,1979,1981, Feeney *et al* 1981, Ortoleva 1987). The dependence of the pulse wave velocity in the BZ-like reaction mixture and of the front wave velocity in the iodate-arsenite reaction on the electric field intensity and on concentrations of reaction components was studied experimentally (Ševčíková and Marek 1983,1984,1986). The process of wave splitting has been recently studied in detail (Ševčíková *et al* 1992). Effects of electric current on spiral waves in the spatially quasi-twodimensional BZ reaction mixture have been studied experimentally (Schütze *et al* 1992, Pérez-Muñuzuri *et al* 1992). The wavelength and the period of spiral waves depend on the electric current intensity and the core of the spiral can be moved by the electric field.

Simplified descriptions of ionic reaction-transport systems based on the assumption of constant electric field intensity valid particularly for solutions of high ionic strength with high mobilities and relatively slow reactions were used until now (Nazarea 1978, Kondepudi 1980, Kondepudi and Prigogine 1981, Almirantis and Nicolis 1987). It was shown, mostly by approximate analytical methods, that weak electrical field can shift the bifurcation points and influence the selection of polar symmetry of stationary spatial patterns. It was also illustrated that the constant electrical field model can describe experimentally observed phenomena in media with high ionic strength (Ševčíková *et al* 1984).

Limitations of the simplified model approach can be evaluated only by comparison with the description based on the considerations of the spatiotemporal distribution of the charge in the medium (Šnita *et al* 1987,1993). The results are particularly important for the understanding of patterns formed in cells and membranes under the influence of both an internally generated and an externally imposed electrical field. In this work we present numerical studies on pattern formation, branch selection and stationary pattern destruction in an ionic version of the Brusselator model located in a one-dimensional reaction-diffusion medium.

1 "Ionic Brusselator" models

The Brusselator reaction scheme assuming electrically charged components can be, for example, written as (Kondepudi 1980, Kondepudi and Prigogine 1981):

$$\begin{aligned} A^+ &\overset{k_1}{\rightleftharpoons} X^+ \\ B^- + X^+ &\overset{k_2}{\rightleftharpoons} Y^+ + D^- \\ 2X^+ + Y^+ &\overset{k_3}{\rightleftharpoons} 3X^+ \end{aligned}$$

$$X^+ \overset{k_4}{\rightleftharpoons} E^+$$

In the course of the paper we will call this scheme "BI1". The same scaling of system variables as in non-ionic Brusselator scheme (Nicolis and Prigogine, 1977) was adopted. The Nernst-Planck equation was used in the balance equations for X and Y to describe their diffusion and migration fluxes. If high ionic strength of the reaction medium is assumed and/or the rates of reactions are moderate the electrical field strength (i.e. the gradient of the potential $\nabla\phi$) may be considered to be approximately constant. The final balance equations then are:

$$\begin{aligned} \frac{\partial X}{\partial \tau} &= A - (B+1)X + X^2Y + D_X(-\nabla X \cdot \nabla\phi + \nabla^2 X) \\ \frac{\partial Y}{\partial \tau} &= BX - X^2Y + D_Y(-\nabla Y \cdot \nabla\phi + \nabla^2 Y) \end{aligned} \tag{1}$$

If the assumption of constant $\nabla\phi$ is not valid both charge balance and local electroneutrality have to be taken into consideration. The scheme BI1 contains not only X^+ and Y^+ but also four additional ions A^+,B^-,D^- and E^+. This makes the rigorous analysis complicated. Hence we used a somewhat simplified scheme BI2. In this scheme only one nonreactive anion C^- is present, formed together with X^+ from an electrically uncharged component A. This also enables us to assume B, D and E to be uncharged components not contributing to the local electric field:

$$\begin{aligned} A &\overset{k_1}{\rightarrow} X^+ + C^- \\ B + X^+ &\overset{k_2}{\rightarrow} Y^+ + D \\ 2X^+ + Y^+ &\overset{k_3}{\rightarrow} 3X^+ \\ X^+ &\overset{k_4}{\rightarrow} X^{+\#} \\ X^{+\#} + C^- &\overset{k_5,\text{fast}}{\longrightarrow} E \end{aligned}$$

We will call this extended Brusselator scheme "BI2". The last two steps ensure that the rate equations for the local chemical kinetics are the same for the original and the above modified scheme. The same scaling as in the original Brusselator was used together with the scaling of C^-:

$$C_C \equiv C = (\frac{k_3}{k_4})^{1/2} c_{C^-}$$

A and B are treated as parameters of the model. At each point of the system the concentration C of the counterion C^- and the value of the current I passing through the system are given by

$$Q = \sum_i Z_i C_i = X + Y - C \doteq 0 \tag{2}$$

$$I = \sum_i Z_i J_i = J_X + J_Y - J_C \tag{3}$$

Here, X and Y denote the dimensionless concentrations of X^+, Y^+; Q is the dimensionless charge $Q = q/(F(k_4/k_3)^{1/2})$ (F: Faraday constant), Z_i is

the charge number of the component i and I is the dimensionless current $I = i/(Fl_0(k_4^3/k_3)^{1/2})$ with l_0 being the characteristic length. The balance equations for X,Y and C are (Šnita *et al* 1993):

$$\begin{aligned} \frac{\partial X}{\partial \tau} &= -\nabla \cdot J_X + A - (B+1)X + X^2Y \\ \frac{\partial Y}{\partial \tau} &= -\nabla \cdot J_Y + BX - X^2Y \\ \frac{\partial C}{\partial \tau} &= -\nabla \cdot J_C + A - X \end{aligned} \tag{4}$$

The charge balance is a linear combination of the balances (4).

$$\frac{\partial Q}{\partial \tau} = -\nabla \cdot I \doteq 0 \tag{5}$$

The current I may be assumed to be constant in a onedimensional system and it provides an additional parameter of the model. The fluxes J_X,J_Y and J_C follow from the Nernst-Planck equation:

$$J_i = -D_i \nabla C_i - Z_i D_i C_i \nabla \phi \tag{6}$$

where D_i is the dimensionless diffusion coefficient of species i. Using Eqs. (2), (3) and (6) the electrical field intensity can be eliminated from the model equations. The balance of C may be expressed in terms of X and Y and the model is completely described by the balances of X and Y and the balance of the charge. The resulting balance equations were solved using a method of the Crank-Nicolson type with adaptive space and time step control. The local electrical field intensity may be calculated as

$$-\nabla \phi = -\frac{I + (D_X - D_C)\nabla X + (D_Y - D_C)\nabla Y}{(D_X + D_C)X + (D_Y + D_C)Y} \tag{7}$$

According to Gauss law of electrostatics the local charge density can be evaluated from the spatial derivative of the electrical field intensity:

$$Q = -\frac{l_D^2}{l_0^2}\nabla^2 \phi \tag{8}$$

where l_D denotes the Debeye length $l_D = ((\epsilon RT)/(F^2(k_4/k_3)^{1/2}))^{1/2}$ and ϵ is the permittivity assumed to be constant due to an excess of solvent. It is well known that the assumption of local electroneutrality (Eq. (2)) is valid for $l_D \ll l_0$.

In the present work we have considered either a spatially one-dimensional system or a two-dimensional rectangular system. We have used boundary conditions of different types and symmetries:

a) Dirichlet boundary conditions with X and Y fixed to their equilibrium values,

b) Dirichlet boundary conditions with X and Y fixed to non-equilibrium values,

c) Dirichlet boundary conditions with asymmetrically fixed boundary concentrations,

d) zero-derivative boundary conditions. In this case, with respect to the Eq.(6), only the migration of ions due to the electric field is allowed at the system boundaries.

2 RESULTS

2.1 Equilibrium boundary values

It is known (Nicolis and Prigogine 1977, Dellnitz *et al* 1991) that the symmetry of patterns generated by the non-ionic classical Brusselator changes with the dimension of the system. Using the actual parameters of this work the classical Brusselator in a spatially one-dimensional system exhibits symmetric Turing patterns up to a length of $L = 0.422$. In larger systems the symmetric solution is unstable and two complementary asymmetric patterns are obtained instead. In the ionic Brusselator (BI2) this symmetry-changing bifurcation is shifted towards higher system sizes. Fig. 1a shows the symmetric solution (thin line) obtained from the ionic Brusselator (BI2) at a system length of $L = 1.375$. Increasing the size of the system creates two complementary asymmetric solutions, one of which is shown in the figure (thick line). The sum of these two newly created solutions exhibits the same symmetry as the previous symmetric pattern. Therefore, the symmetric solution may be considered to arise from the collision of the two asymmetric patterns. All these patterns differ with respect to their fluxes at the boundaries, i.e. in the way they interact with their environment. Whereas the fluxes for the symmetric pattern are of opposite sign but equal magnitude at the boundaries, the fluxes of the asymmetric patterns posess equal sign and differ in magnitude. For a system of length L=1.40 the fluxes of, e.g., X at the boundaries of the unstable symmetric pattern are $J_{left} = 4.52 * 10^{-2}$ and $J_{right} = -4.52 * 10^{-2}$, for the stable asymmetric patterns the fluxes $J_{left} = -2.70 * 10^{-2}$ and $J_{right} = -4.26 * 10^{-2}$ (vice versa for the second pattern) are found. Hence the bifurcation into asymmetric patterns is connected with an approximately two-fold decrease of the flux at one of the boundaries of the membrane.

In Fig. 1b,c the profiles of the electrical field intensity and of the charge density derived from the symmetric profile in Fig. 1a are displayed. The different mobilities of the ionic compounds generate internal inhomogeneities of the electrical field and of the charge density even in the absence of an external electrical field. These inhomogeneities strongly affect the transport of ions in the system.

An external electric current of the strength $I = \pm 2.5$ destabilizes one of the two complementary patterns mentioned above and only one solution is obtained, no matter to which of the two profiles the current is applied. The direction of the current determines which pattern is favored (cf. Fig. 2). The patterns are somewhat distorted by the external field and the fluxes of X at the boundaries are $J_{left} = -2.63 * 10^{-2}$ and $J_{right} = -4.25 * 10^{-2}$ and vice versa, mainly dominated by the diffusive contribution to the transport rather than by the electrical one. This clearly demonstrates that the switch between mutually symmetric patterns caused by a weak electrical field is reflected in a large change of the flux in or out of the system. The distorted patterns are stationary until the current reaches a value of $I = \pm 4.9$.

The effect of increasing ionic strength of the reaction medium can be investigated by adding a nonreactive cation K^+ with the same diffusivity as C^- to the scheme BI2. The concentration of the negative counterion C^- is

then given by $C = X + Y + K$, where X, Y and K represent the dimensionless concentrations of X^+, Y^+ and K^+. In this case, increasing the boundary values of K will increase the ionic strength in the system and decrease the spatial variations of the internal electrical field. Without an externally applied electrical field the simple model (Eq. (1)) shows the sharper profile shown in Fig. 3 (light line). The corresponding profile obtained from the full model BI2 with $K = 0$ is shown in the same figure (heavy line). As the value of K at the boundaries is increased, the pattern for the full model BI2 approaches the pattern formed in the simple model at $K(0) = K(L) = 8.5$. This numerical experiment demonstrates that the simplified model may be viewed as a special case of the full model description valid for high ionic strength, high mobility of ions and moderate reaction rates.

2.2 Asymmetrically fixed boundary values

In biological systems membranes commonly separate compartments of different composition and their boundaries display only low symmetry. We therefore performed numerical simulations with asymmetrically fixed boundary conditions At $L = 0$ the intermediates X and Y were kept at their equilibrium values A and B/A, respectively. The second boundary, however, was considered to be connected to a domain where X and Y can only reach 75% of their equilibrium values. Without an externally applied current two patterns coexist which differ in the fluxes at their boundaries.

Fig. 4a,b shows the two patterns obtained with the non-ionic classical Brusselator and Fig. 4c,d displays the corresponding solutions of the full ionic model BI2 without an external electrical field. It is seen that the wavelength of the pattern increases if charged intermediates are assumed. For one solution also the wavenumber decreases if the intermediates are charged. In Fig. 5 the fluxes at the boundaries are drawn as a function of the current driven through the system.The fluxes at $L = 2$ only slightly and almost linearly increase with the current. In the vicinity of the boundary at $L = 0$ the effects of the current are larger. At low values of the current the two patterns of Fig. 4c,d still coexist though they get more and more distorted as the absolute value of the current increases. Beyond a certain threshold value of the current in either direction ($I_{th}^- = -2.95$ and $I_{th}^+ = 2.13$) the pattern with negative fluxes at the boundaries disappears and only one solution is obtained. Further increase of the current leads to travelling waves. The simple model does not show any oscillations induced by the electrical field.

2.3 Zero-derivative boundary conditions

Using zero-diffusion flux boundary conditions the classical non-ionic Brusselator with the parameters used in this work undergoes a Turing bifurcation at the critical value of $B_c = 4.132...$ At lower values of B only flat profiles of X and Y are formed. Assuming the scheme BI1 (Eq. (1)) the value of B_c decreases if an electrical field is applied. Asymmetrically distorted stationary patterns now develop even at values of $B < B_c$. The new critical value B_c^e is decreased as $-\nabla\phi$ increases. The same conclusion had been obtained earlier (Nazarea 1978, Kondepudi 1980, Kondepudi and Prigogine 1981) by an application of approximate analytical method. In Fig. 6 the response of the patterns to an externally applied electrical field is displayed for Eq. (1). The

wavelength of the pattern increases with the electrical field and the peaks corresponding to high concentration of X are shifted out of the system at the left boundary. Correspondingly, the concentration of X and Y at this boundary will vary with the field in an almost cyclic manner as consecutive peaks are shifted over the boundary. The fluxes of X at the boundaries are shown in Fig. 7. While the flux increases monotonically with the external field at one boundary, it alternates at the second. Again, no oscillatory behaviour was induced by the external field.

When the full model for the scheme BI2 is solved with the zero-diffusional flux boundary conditions the following types of system behaviour can be observed:

At low values of the parameter B steady spatial patterns are evoked by the nonzero electric current passing through the membrane, even for values of B at which only spatially homogeneous steady state exists under the zero current or in the non-ionic Brusselator. The critical value B_c is remarkably lowered in the ionic system with current passing through the system compared to the critical values of non-ionic Brusselator (Nicolis and Prigogine 1977). The patterns evoked by the current are strongly asymmetric. These results are in qualitative agreement with predictions derived for the simplified model with constant electric field intensity $-\nabla\phi$ (Kondepudi 1980, Kondepudi and Prigogine 1981).

At moderate and high values of B the steady patterns generated inside the membrane are symmetric when no current passes through. When increasing the current intensity the patterns are more and more distorted. At even higher intensity of the current the temporal oscillations arise in the system. The coexistence of the spatially steady pattern region with the region of bulk oscillations generated by the current of magnitude $I = +10$ is shown in Fig. 8. The width of the oscillating region increases with increasing current value. Similar behaviour was observed in a 2-D BZ reaction system modelled with the simplified model equations (Steinbock *et al* 1991). The current of magnitude $I = -10$ applied to the same system generates quite different behaviour, cf. Fig. 9. In this case trains of pulse waves evolve near the left boundary moving, after the transients have died out, with constant velocity to the right boundary, where they are annihilated. The width of the region with travelling waves again depends on current value.

Response of the ionic Brusselator (scheme BI2, full model formulation) to the periodic forcing with alternating electric current was simulated too (cf. Fig.10). The well developed dissipative structure with the wavenumber $m = 7$ exists in the system. This structure is only slightly disturbed by the alternating current. The temporal oscillations at any point inside membrane are damped, only at the boundaries the amplitude of the oscillations is more pronounced. The oscillations inside the membrane are synchronized with the period of the forcing current.

2.4 The Twodimensional System

We assumed high ionic strength of the medium, moderate reaction rates and comparable mobilities of the charged particles. Thus our calculations are based on scheme BI1 and Eq. (1) adding a further term for the diffusion in the second spatial coordinate in a plane. Diffusion coefficients are assumed to be equal in both directions, the electrical field is constant throughout the

whole system and its direction is parallel to r_2. There is no component of the electrical field parallel to the second spatial dimension r_1. The values of X and Y were fixed at their equilibrium values at $r_2(0)$ and $r_2(1)$ and to 0 at $r_1(0)$ and $r_1(1)$ respectively. In Fig. 11a the pattern generated at the absence of an external field is shown. Fig. 11b presents a stationary pattern obtained at an external field strength of $-\nabla\phi = 20$. It is seen that the wavenumber is decreased by the action of the external field, the wavelength along r_2 has increased and the shape of the spots has changed from a mixture of hexagons and stripes into stripes. Similar changes have been observed in experiments (Ouyang and Swinney 1991).

3 Discussion

The formation of stationary spatial patterns by the interaction of a nonlinear chemical reaction mechanism with transport of reaction components in a distributed system is believed to play a crucial role in biological morphogenesis. Stationary pattern formation in a distributed system is a well studied phenomenon in the classical Brusselator model (Kevrekidis and Brown 1989, Boissonade 1988, Dewel and Borckmans 1989, Borckmans *et al* 1992). In order to study the influence of electrical field on such "Turing-patterns" we have chosen two different approaches of introducing electrical charge to the model. In each case the rate equations describing the classical Brusselator are extended by an expression for the transport of ionic compounds according to the Nernst-Planck equation. The simple approach assumes a spatially constant electrical field whereas the local electrical field intensity in the more complex approach is derived from the Poisson equation and it therefore can exhibit inhomogeneities in space. Such spatial variations of the field may be generated by the different mobilities of the ions present in the reaction mixture. The latter approach requires to include a nonreactive counterion into the reaction scheme. Without an externally applied electrical field the patterns obtained from the two models differ in their amplitudes and wavelengths. The full model including spatial variations of the field yields concentration profiles of smaller amplitudes and larger wavelengths than the simplified model which neglects internally generated electrical field inhomogeneities. Using fixed boundary values both models posess multiple solutions which differ in their symmetry. Accordingly, the fluxes these patterns exhibit at their boundaries differ. At small intensities of an externally imposed electrical field the concentration patterns are distorted by the field in both models considered. In the case of fixed boundary values with at least one boundary fixed to equilibrium values of X and Y there is a region of hysteresis if the external electrical field intensity is shifted up and down. Here two different patterns coexist and it depends on the initial conditions which pattern will form. This hysteresis is also reflected by the fluxes at the system boundaries. The system therefore "remembers" its initial conditions and the fluxes at the boundaries sensitively depend on them. At the limits of the hysteresis region small changes in the external electrical field strength may lead to large changes in the fluxes by switching from one pattern to another. A nonlinear dependence of the fluxes at the boundaries on the external electrical field is also observed under zero-derivative boundary conditions. Furthermore, under these conditions the critical value B_c of the parameter B, where the pattern formation sets on, is decreased in both the

full and the simplified model. While both models show qualitatively similar behaviour at low values of the externally imposed electrical field intensity they differ remarkably at higher values of the external field. In the simplified model the distortion of the patterns continues and the fluxes at the boundaries vary in an almost cyclic fashion with increasing electrical field intensity. In the complex model, however, the stationary patterns turn into travelling waves or bulk oscillations as the external field exceeds a certain threshold value. Correspondingly, the fluxes at the boundaries begin to oscillate. The amplitude of these oscillations of the fluxes is large if X and Y are fixed to their equilibrium values or if zero-derivative boundary conditions are used. In the latter case a region of travelling waves exists spatially separated from a region of almost stationary behaviour. Therefore the fluxes are almost constant at one boundary and oscillatory at the other. If X and Y are fixed to non-equilibrium values at both boundaries, large oscillations occur in the interior of the system but the fluxes at the boundaries oscillate with only small amplitudes.

Spatial and/or spatiotemporal charge distribution varies greatly on the scale of the characteristic pattern size. We can speculate that such large variations would affect both tertiary and quarternary structure of proteins present in biological membranes. Enzymatic activity of such proteins could then be strongly affected too. This would have implications, e.g. for a prepattern formation and control in morphogenesis.

4 References

Almirantis Y., Nicolis G. 1987. *Bull. Math. Biol.* 47, 519.

Almirantis Y., Kaufman M. 1992. *Int. J. Bif. Chaos* 2, 51.

Boissonade J. 1988. *J. Phys. France* 49, 541.

Borckmans P., De Wit A., Dewel G. 1992. *Physica A* 188, 137.

Castets V. , Dulos E., Boissonade J., DeKepper P. 1990.*Phys. Rev. Lett.* 64, 2953.

Dellnitz M., Golubitsky M., Melbourne I. 1991. *Research-Report UH/MD-114.* Department of Mathematics, University of Houston. Texas.

Dewel G., Borckmans P. 1989. *Phys. Lett. A* 138, 189.

Feeney R., Schmidt S., Ortoleva P. 1981. *Physica D* 2, 536.

Kevrekidis I. G., Brown H. S. 1989. *Chem. Eng. Sci* 44, 1893.

Kondepudi D. K. 1980. *Phys. Lett. A* 77, 203.

Kondepudi D. K., Prigogine I. 1981. *Physica A* 107, 1.

Kshirsagar G., Noszticzius Z., McCormick W. D., Swinney H. L. 1991. *Physica D* 49, 5.

Nazarea A.D. 1978. *Adv. Chem. Phys.* 38, 415.

Nicolis G., Prigogine I. 1977. *Self-Organisazion in Nonequilibrium Systems* John Wiley & Sons: New-York, London, Sidney, Toronto.

Noszticzius Z., Horsthemke W., McCormick W. D., Swinney H. L., Tam W. Y. 1987. *Nature* 329, 619.

Ortoleva P. 1987. *Physica D* 26, 67.

Ouyang Q., Swinney H. L. 1991a. *Nature* 352, 610.

Ouyang Q., Swinney H. L. 1991b. *Chaos* 1, 411.

Pérez-Muñuzuri V., Aliev R., Vasiev B., Krinsky V.I. 1992. *Physica D* 56, 229.

Schmidt S., Ortoleva P. 1977. *J. Chem. Phys.* 67, 3771.

Schmidt S., Ortoleva P. 1979. *J. Chem. Phys.* 71, 1010.

Schmidt S., Ortoleva P. 1981. *J. Chem. Phys.* 74, 4488.

Schütze J., Steinbock O., Müller S. C. 1992. *Nature* 356, 45.

Steinbock O., Schütze J., Müller S. C. 1991. *Phys. Rev. Lett.* 68, 248.

Ševčíková H., Marek M. 1983. *Physica D* 9, 140.

Ševčíková H., Marek M. 1984. *Physica D* 13, 379.

Ševčíková H., Marek M. 1986. *Physica D* 21, 61.

Ševčíková H., Marek M., Müller S. C. 1992. *Science* 257, 951.

Ševčíková H., Kubíček M., Marek M. 1984. Concentration waves - effects of an electric field. In: *Mathematical Modelling in Sciences and Technology.* X.J.R. Avula, A.I. Ljapis, E.Y. Rodin (Eds.) p. 417, Pergamon Press, New York.

Šnita D., Marek M. 1987. Interaction of electromagnetic field with enzymatic reactions and pH effects. In: *Horizons of Biochemical Engineering* S. Aiba (Ed.), 337-365. University of Tokyo Press.

Šnita D., Dvořák L., Marek M. 1993. submitted to *Physica D*

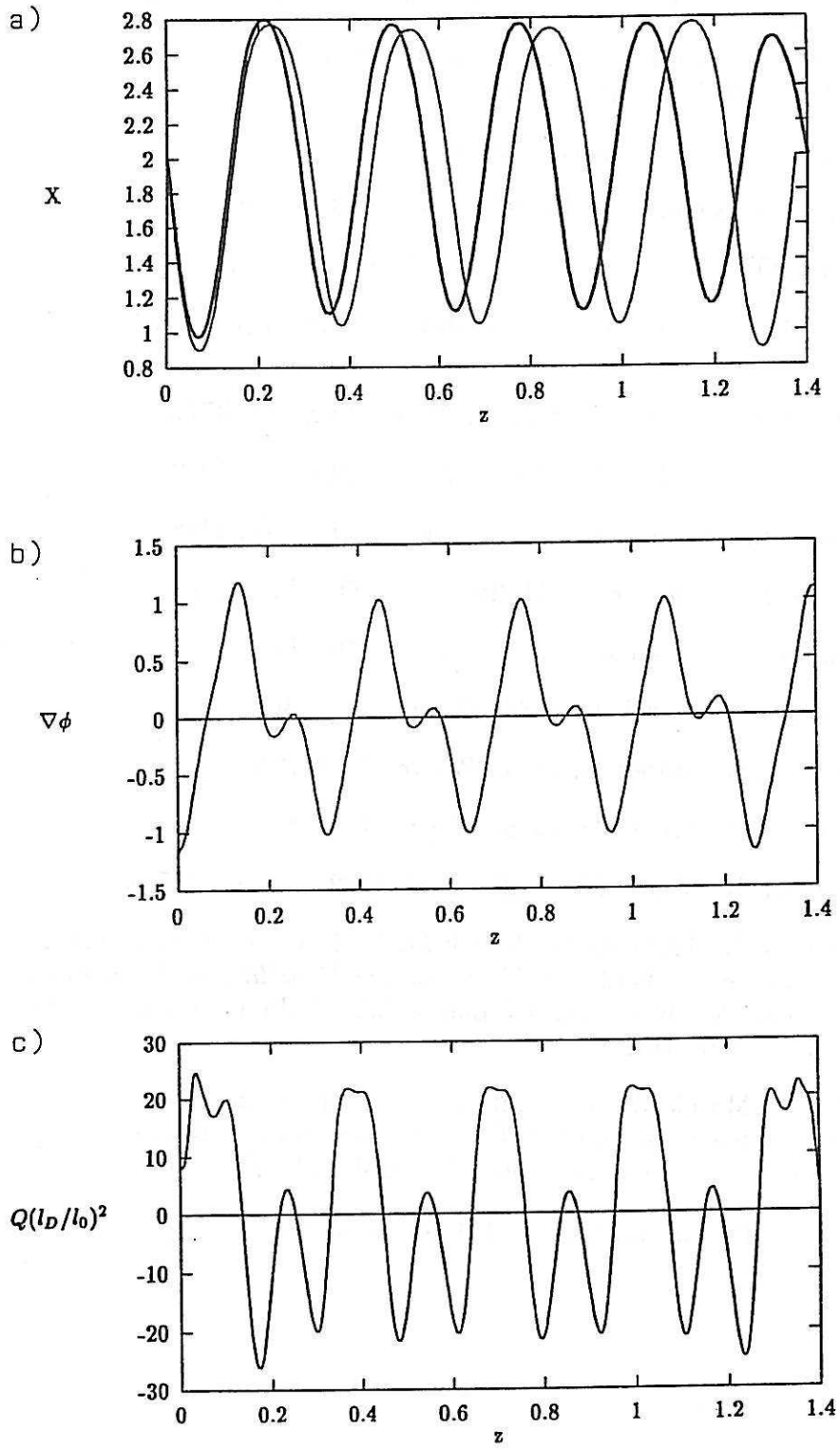

Figure 1: a) Symmetric and asymmetric profiles obtained at system lengths $L = 1.375$ and $L = 1.400$. b) Profile of the local electrical field intensity corresponding to the symmetric pattern in Fig.1a. c) The charge density profile corresponding to the symmetric pattern in Fig.1a. The ionic Brusselator scheme BI2, full model. Parameters: $A = 2.0$, $B = 5.2$, $D_X = 1.6 \cdot 10^{-3}$, $D_Y = 6.0 \cdot 10^{-3}$, $D_C = 1.0$

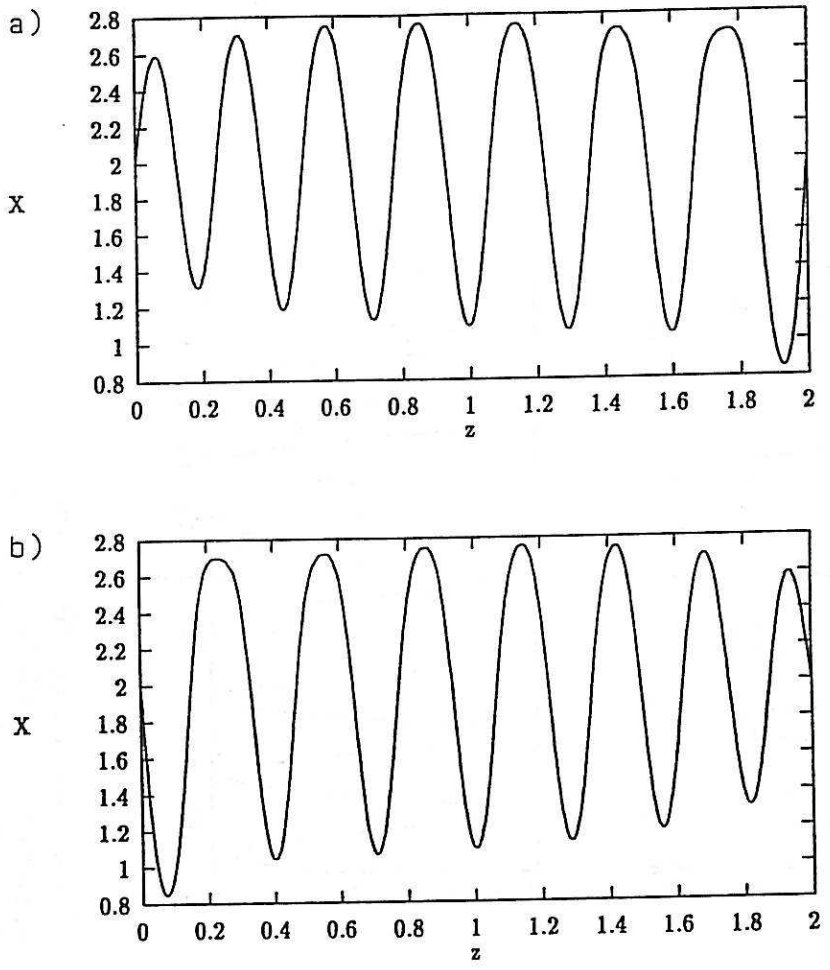

Figure 2: Asymmetric concentration profiles of X. a) Current $I = +2.5$, b) current $I = -2.5$ The ionic Brusselator scheme BI2, full model. Parameters: $A = 2.0$, $B = 5.2$, $L = 2$, $D_X = 1.6 \cdot 10^{-3}$, $D_Y = 6.0 \cdot 10^{-3}$, $D_C = 1.0$

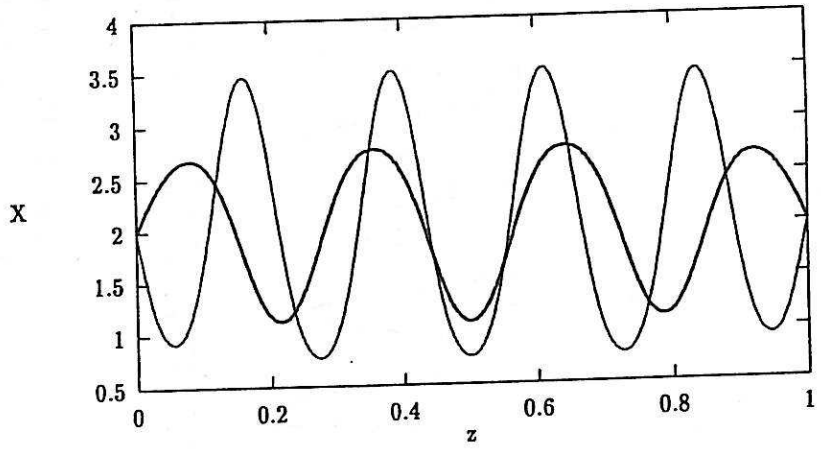

Figure 3: Comparison of models BI1 (light line) and BI2 (heavy line). When the concentration of a nonreactive counterion K^+ is increased, the profile for BI2 model grows in amplitude; beyond a threshold value of K^+ concentration it switches to a profile similar to the one obtained from BI1 scheme. Further increase of K^+ concentration increases the amplitude of the BI2 profile until it becomes practically identical to the BI1 profile. Parameters: $A = 2.0$, $B = 5.2$, $L = 1.0$, $D_X = 1.6 \cdot 10^{-3}$, $D_Y = 6.0 \cdot 10^{-3}$, $D_C = 1.0$

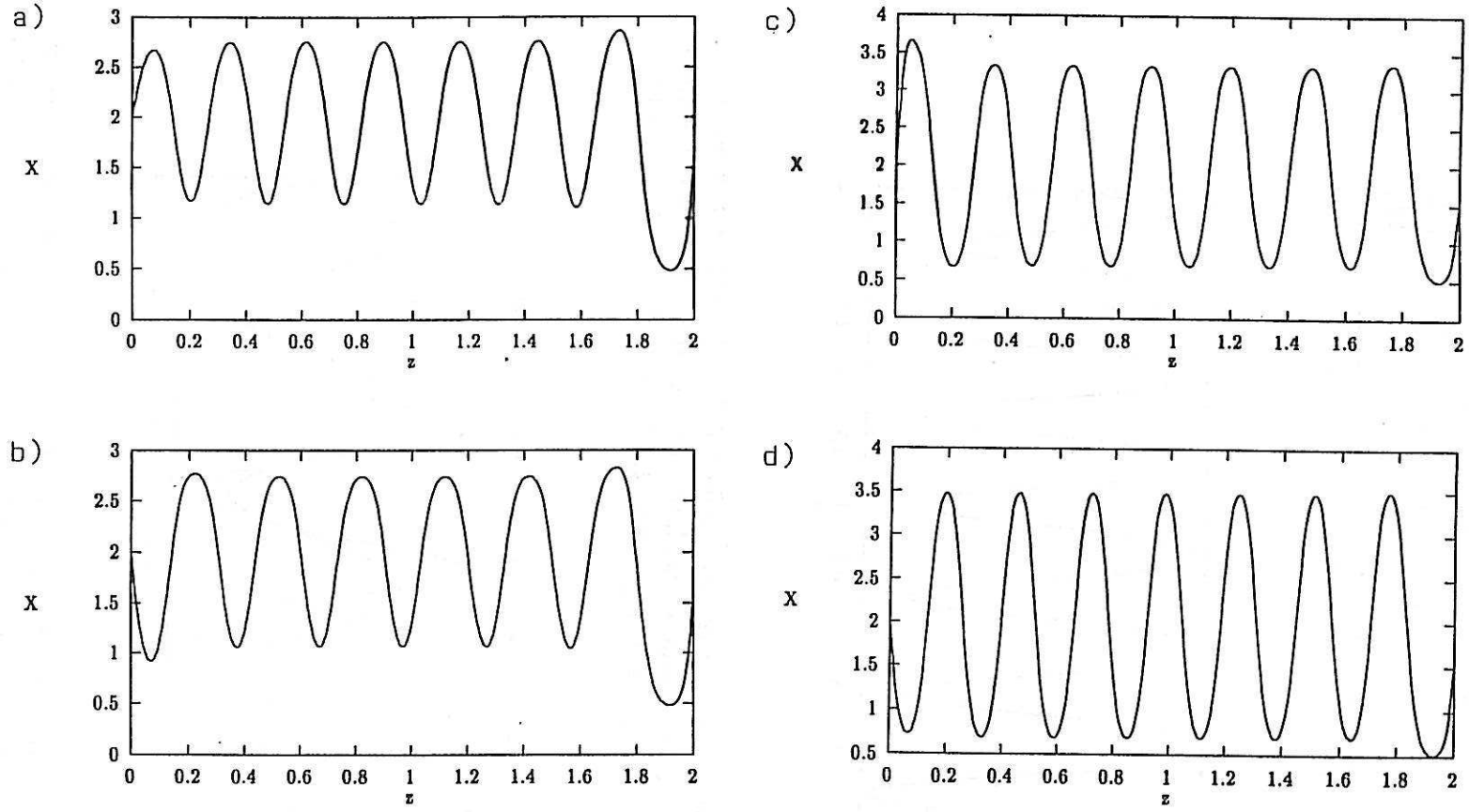

Figure 4: Coexisting stable profiles in the Brusselator models with asymmetrically fixed boundary concentrations. **a)** and **b)**: non-ionic Brusselator, **c)** and **d)**: the ionic Brusselator scheme BI2, full model. Boundary values: $X(0) = 2.0, X(2) = 1.5, Y(0) = 2.6, Y(2) = 1.95$. No external current (field) applied. Parameters: $A = 2.0$, $B = 5.2$, $L = 2.0$, $D_X = 1.6 \cdot 10^{-3}$, $D_Y = 6.0 \cdot 10^{-3}$, $D_C = 1.0$

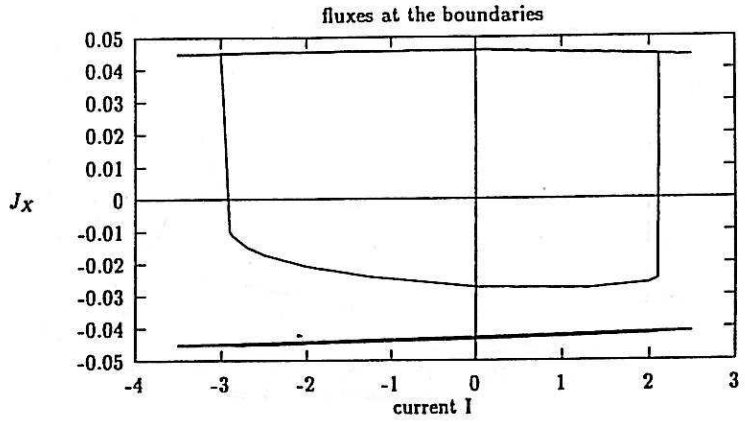

Figure 5: Fluxes of the component X in the model BI2 at the boundaries as a function of the current driven through the system. Boundary concentrations: $X(0) = 2.0, Y(0) = 2.6, X(L) = 1.5, Y(L) = 1.95$. The boundary $z = 0$ shows hysteresis of the flux, the flux at boundary $z = L$ is practically constant. Parameters: $A = 2.0$, $B = 5.2$, $L = 2.0$ $D_X = 1.6 \cdot 10^{-3}$, $D_Y = 6.0 \cdot 10^{-3}$, $D_C = 1.0$

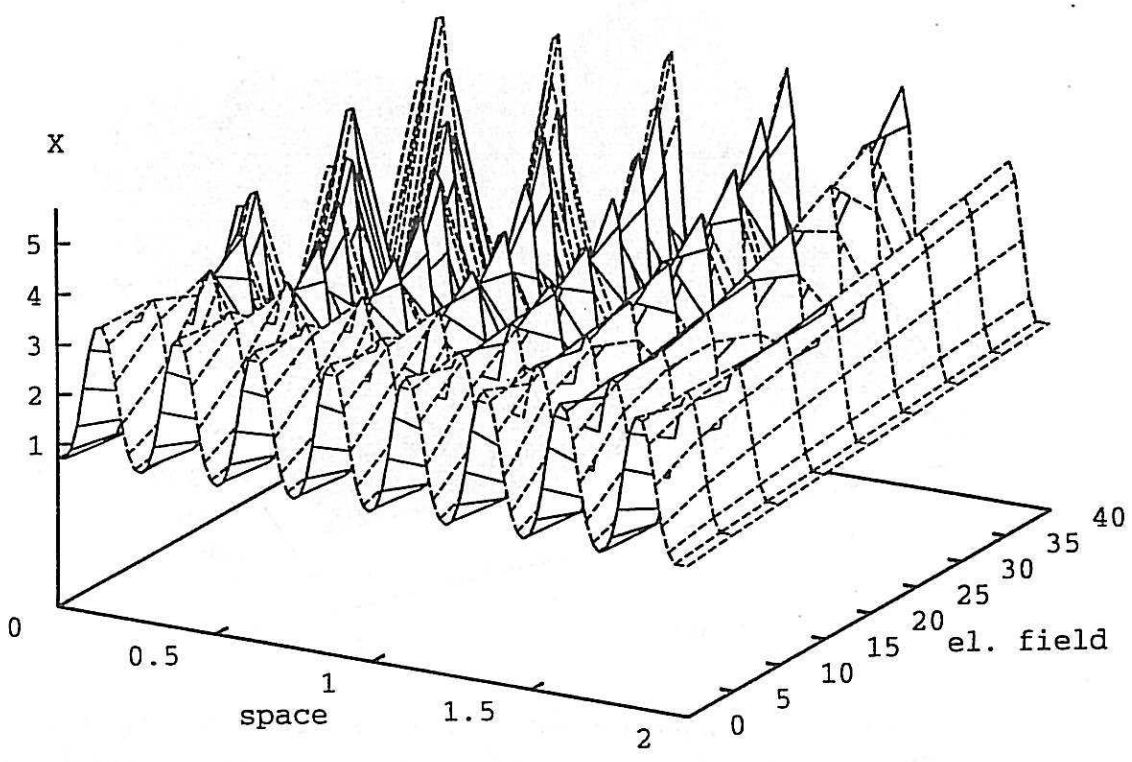

Figure 6: Distortion of concentration pattern obtained from the simplified model BI1 with zero-derivative boundary conditions under the increasing electrical field strength $-\nabla\phi$. Parameters: $A = 2.0$, $B = 5.2$, $D_X = 1.6 \cdot 10^{-3}$, $D_Y = 6.0 \cdot 10^{-3}$, $D_C = 1.0$

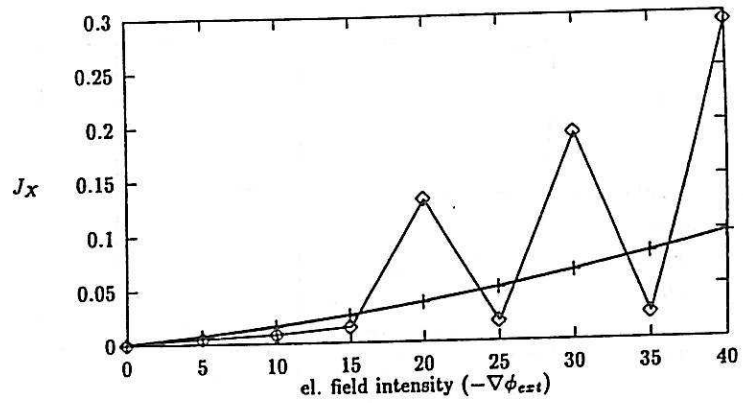

Figure 7: Fluxes at the boundaries for the simplified model BI1 with zero-derivative boundary conditions as a function of the externally applied electrical field intensity. The light line refers to the boundary $z = 0$, the heavy line to the one at $z = 2.0$. Parameters: $A = 2.0$, $B = 5.2$, $D_X = 1.6 \cdot 10^{-3}$, $D_Y = 6.0 \cdot 10^{-3}$, $D_C = 1.0$

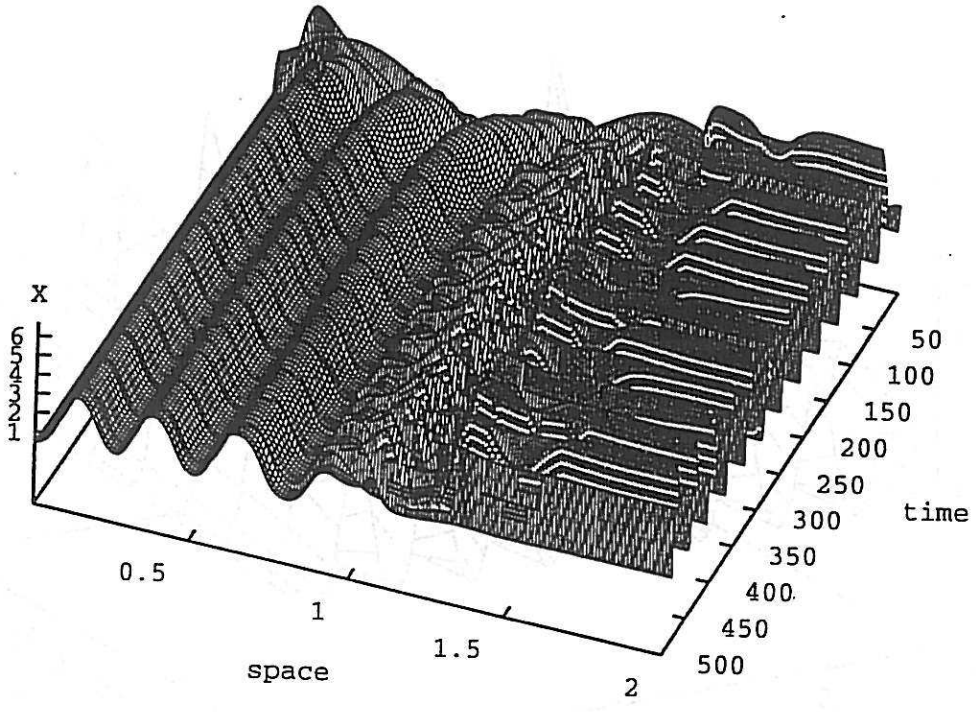

Figure 8: Spatiotemporal evolution of coexisting steady pattern and bulk oscillations inside the system starting from $X_0 = 2sin(4\pi z/L) + 1, Y_0 = B/A$. Current $I = +10.0$ The ionic Brusselator scheme BI2, full model. Parameters: $A = 2.0$, $B = 5.2$, $L = 2$, $D_X = 1.6 \cdot 10^{-3}$, $D_Y = 6.0 \cdot 10^{-3}$, $D_C = 1.0$

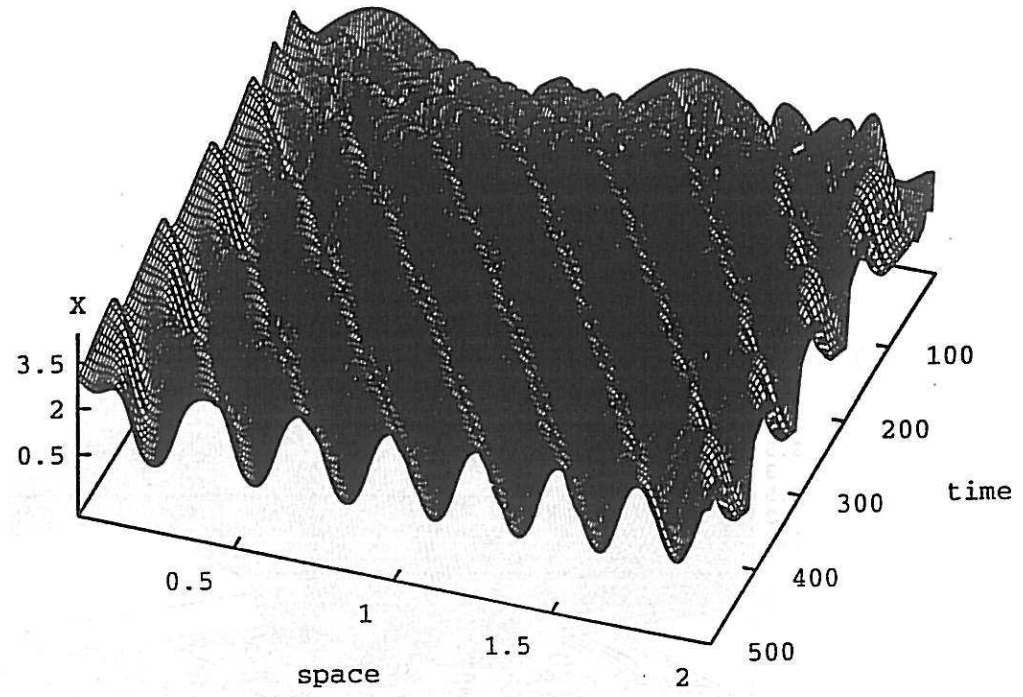

Figure 9: Spatiotemporal evolution of travelling pulse waves inside the system starting from the profiles $X_0 = 2sin(4\pi z/L) + 1, Y_0 = B/A$. Current $I = -10.0$. The ionic Brusselator scheme BI2, full model. Parameters: $A = 2.0$, $B = 5.2$, $L = 2$, $D_X = 1.6 \cdot 10^{-3}$, $D_Y = 6.0 \cdot 10^{-3}$, $D_C = 1.0$

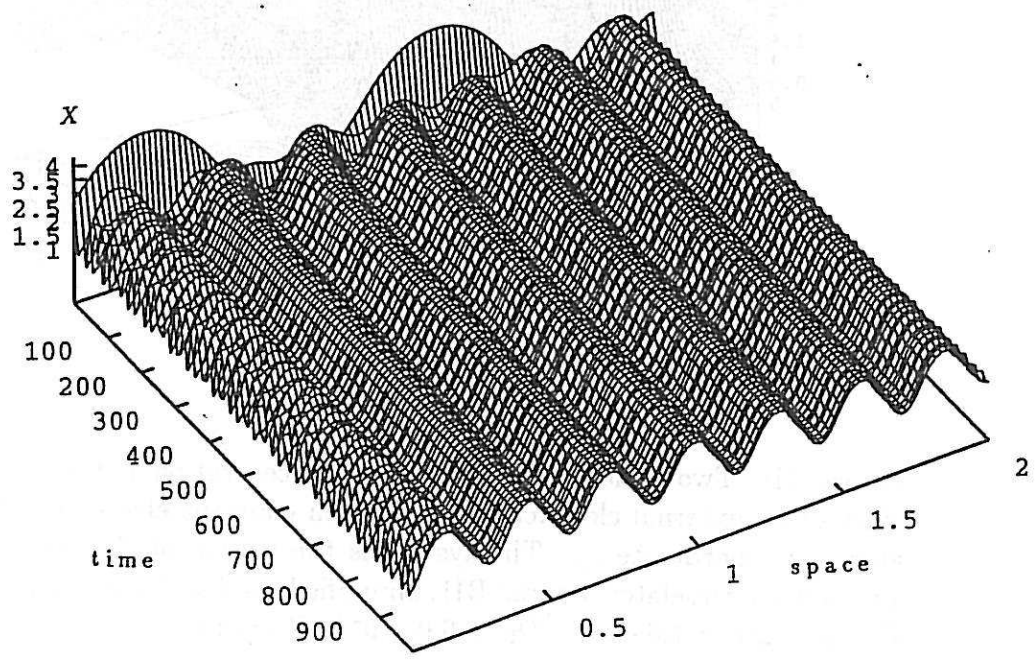

Figure 10: Spatiotemporal evolution of response to the alternating current forcing starting from $X_0 = 2sin(4\pi z/L) + 1, Y_0 = B/A$. Current $I = I_0 sin(\omega t)$ The ionic Brusselator scheme BI2, full model. Parameters: $A = 2.0$, $B = 5.2$, $L = 2$, $D_X = 1.6 \cdot 10^{-3}$, $D_Y = 6.0 \cdot 10^{-3}$, $D_C = 1.0$ $I_0 = +5.0$, $\omega = 0.25$

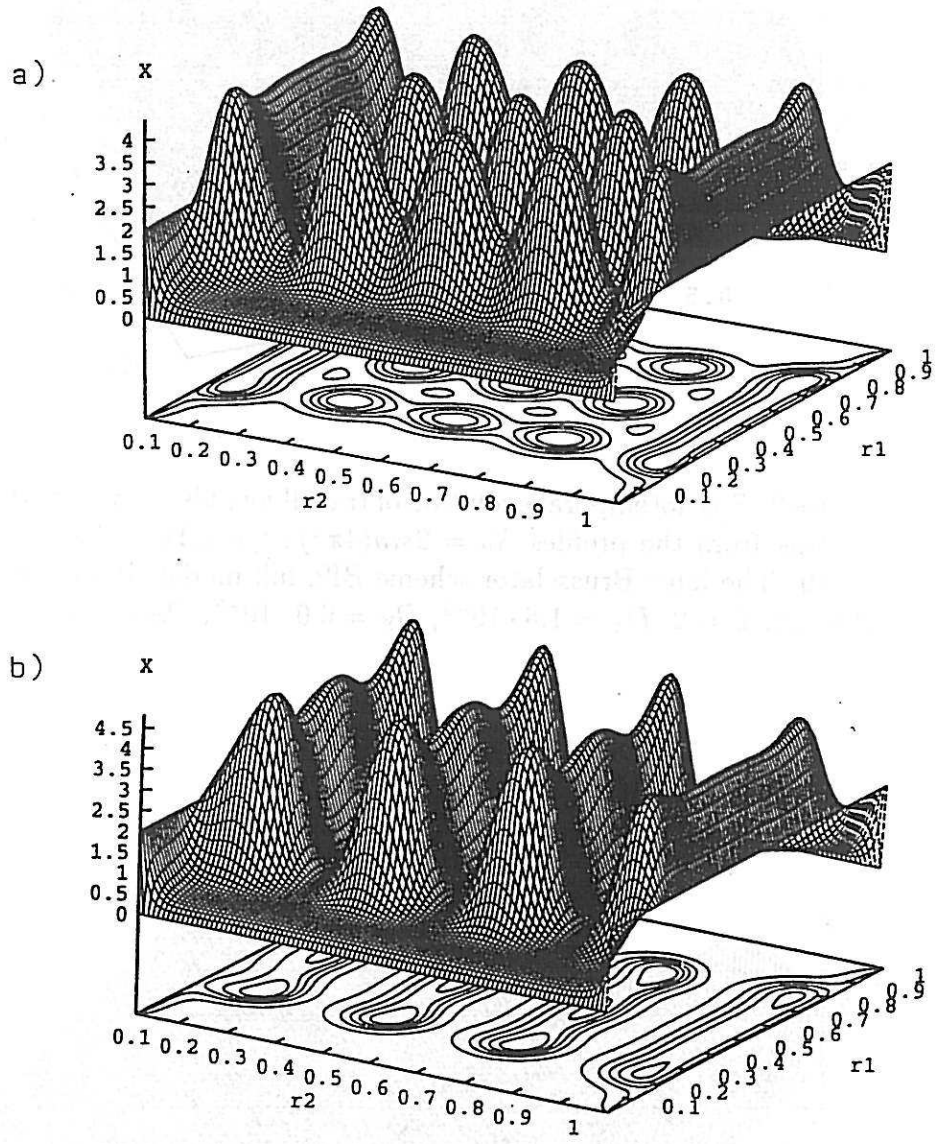

Figure 11: Two-dimensional stationary concentration patterns of X. **a)** without an external electrical field, **b)** with constant electrical field applied along the coordinate r_2. The system is the square of the size: 1.0×1.0. The ionic Brusselator scheme BI1, simplified model. Parameters: $A = 2.0$, $B = 5.2$, $D_X = 1.6 \cdot 10^{-3}$, $D_Y = 6.0 \cdot 10^{-3}$, $D_C = 1.0$